**Ambiente & Água - An Interdisciplinary Journal of Applied Science**
ISSN 1980-993X – doi:10.4136/1980-993X
www.ambi-agua.net
E-mail: ambi.agua@gmail.com

# Sediment dynamics in a semiarid catchment with cascade dam failures

**ARTICLES doi:10.4136/ambi-agua.3122**

**Received: 12 Sep. 2025; Accepted: 28 Oct. 2025**

**George Leite Mamede*; Jued Lomba Purna;**
**Sandy Kelly Monteiro De Menezes; Emilly Martins Silveira**

Instituto de Engenharias e Desenvolvimento Sustentável. Universidade da Integração Internacional da Lusofonia Afro-Brasileira (UNILAB), Campus das Auroras, Rua José Franco de Oliveira, s/n, CEP: 62790-970, Redenção, CE, Brazil. E-mail: jued@aluno.unilab.edu.br, sandyfemo@gmail.com, emillymartinssilveira@gmail.com
*Corresponding author. E-mail: mamede@unilab.edu.br

**Editor-in-Chief: Nelson Wellausen Dias**

## ABSTRACT

The research estimates the risks of cascade dam failures in a network of fifteen reservoirs in the Nogueira River Basin and their effects on sediment mobilization from the dam embankments. The runoff simulation was performed using the HEC-HMS model for the IDF curve of the Pentecoste meteorological station and different return periods. The hydraulic modeling of the cascade dam failure was performed using HEC-RAS. The results indicate that high flows with return periods exceeding 100 years can result in cascade dam failures. In the most extreme flood event, with a return period of 10,000 years, thirteen dams would fail, mobilizing substantial amounts of water and sediments. The results also highlight the ability of larger reservoirs to attenuate flood waves resulting from the failure of smaller dams located downstream. Nevertheless, they are still subject to failure during more extreme events (1,000 and 10,000 years). Regarding sediment dynamics, the results show significant sediment mobilization from the dam embankments during cascade dam failures. In the simulation for the 10,000-year return period, sediment erosion from dam embankments is observed to be thirteen times greater than that produced in the river basin, with negative impacts downstream. The effects of cascade dam failures on sediment dynamics are also analyzed in terms of average sediment concentrations at the reservoir inlet and outlet. The results indicate abrupt changes in the values of this variable due to the large amount of sediments eroded from the dam embankments and transported downstream in the reservoir network.

**Keywords:** breach formation, cascading dam failure, flood events.

# Dinâmica de sedimentos em uma bacia hidrográfica semiárida com ruptura de barragens em cascata

## RESUMO

A pesquisa tem como objetivo estimar os riscos de ruptura de barragens em cascata em uma rede de quinze reservatórios da bacia hidrográfica do rio Nogueira e seus efeitos na mobilização de sedimentos do corpo do maciço. A simulação do escoamento superficial foi realizada com o modelo HEC-HMS para a curva IDF da estação meteorológica de Pentecoste e diferentes períodos de retorno. A modelagem hidráulica da ruptura das barragens em cascata foi realizada com o HEC-RAS. Os resultados indicam que vazões elevadas com períodos de retorno superiores a 100 anos podem resultar em ruptura de barragens em cascata. No evento de cheia mais extremo, com período de retorno de 10.000 anos, treze barragens romperiam, mobilizando grandes quantidades de água e sedimentos. Os resultados também destacam a capacidade dos reservatórios maiores em atenuar ondas de cheia resultantes de ruptura de barragens menores localizadas a jusante. No entanto, ainda estão sujeitos a ruptura para eventos mais extremos (1.000 e 10.000 anos). Com relação à dinâmica de sedimentos, os resultados mostram uma grande mobilização de sedimentos dos maciços de terra em rupturas de barragens em cascata. Na simulação para o período de retorno de 10.000 anos, observa-se uma erosão de sedimentos dos aterros das barragens treze vezes superior ao que é produzido na bacia hidrográfica, com impactos negativos a jusante. Os efeitos da ruptura de barragens em cascata na dinâmica de sedimentos também são analisados em termos das concentrações médias de sedimentos na entrada e saída dos reservatórios. Os resultados indicam mudanças abrutas nos valores desta variável como resultado da grande quantidade de sedimentos erodidos dos aterros das barragens e transportados para jusante na rede de reservatórios.

**Palavras-chave:** eventos de cheia, formação da fenda, ruptura de barragens em cascata.

## 1. INTRODUCTION

The Brazilian semi-arid region is characterized by a high-intensity and short-duration rainfall concentrated in a few months of the year. Thus, the construction of dense networks of surface reservoirs has been adopted as an alternative for water storage during rainy periods and water supply during dry periods (Mamede *et al.*, 2012; 2018; de Araújo and Medeiros, 2013; Peter *et al.*, 2014). The state of Ceará has a dense network of surface reservoirs, most of which are small- and medium-sized with storage capacities of less than 1 hm³, arranged in cascades (Maia *et al.*, 2025). These small dams are often built without hydraulic and hydrological studies of extreme events to size the spillway and earth massif and without analyzing the stability of slopes, leaving the structure more prone to the occurrence of ruptures and appearance of fissures and infiltrations, among other problems (Gomes, 2019).

According to the Brazil Dam Safety Report (ANA, 2025), 153 dam failures were recorded between 2011 and 2024. In the last two years (2023 and 2024), 49 dam accidents occurred, 13 of which were in the State of Ceará (26.5% of cases). Most of the failures were caused by overtopping associated with extreme flood events, including some records of cascading dam failures (12 dams).

Several authors have developed studies on dam failure and downstream flood wave propagation in recent decades (Zhao *et al.*, 2017; Vosoughi *et al.*, 2020). On the other hand, some investigations into the flow and transport of sediments due to the failure of an embankment dam (Zhang and Wu, 2011; Taskaya *et al.*, 2023) and tailing dam (Chen and Cunning, 2025; Mello and Eleutério, 2025) are also found. Other studies have focused on cascade dam failure using a scaled physical representation of the prototype system (Qiu *et al.*, 2024; Fu *et al.*, 2025) or hypothetical failures of real dams arranged in cascade (Oliveira and Lima Neto, 2022; Campos and Saliba, 2023). Nevertheless, none of them have investigated the failure risk analysis of cascade dams in dense networks of small reservoirs, which is an important issue in the Semiarid region of Ceará.

This study, therefore, focused on the simulation of dam failure risks in a network of 15 reservoirs in the Brazilian Semiarid region and estimated the amount of sediment mobilized from the watershed and the earth-fill dam body during flood events with cascade dam failures.

# 2. MATERIAL AND METHODS

The study area is located within the Curu River Basin (Figure 1), including: the Experimental Basin of the Curu Valley (EBCV), belonging to the Federal University of Ceará, with a contributing area of 2.6 km²; and the Nogueira River Basin (NRB), located on the left bank of the Canindé River, the main tributary of the Curu River, with a catchment area of 31.6 km². The NRB has a network of 15 reservoirs for water storage, with water surface areas ranging from 0.23 to 54.9 ha and storage volumes ranging from 574 m³ to 2 million m³. The largest reservoir named Carrapato is located at the catchment outlet (reservoir ID-4, according to Figure 1).

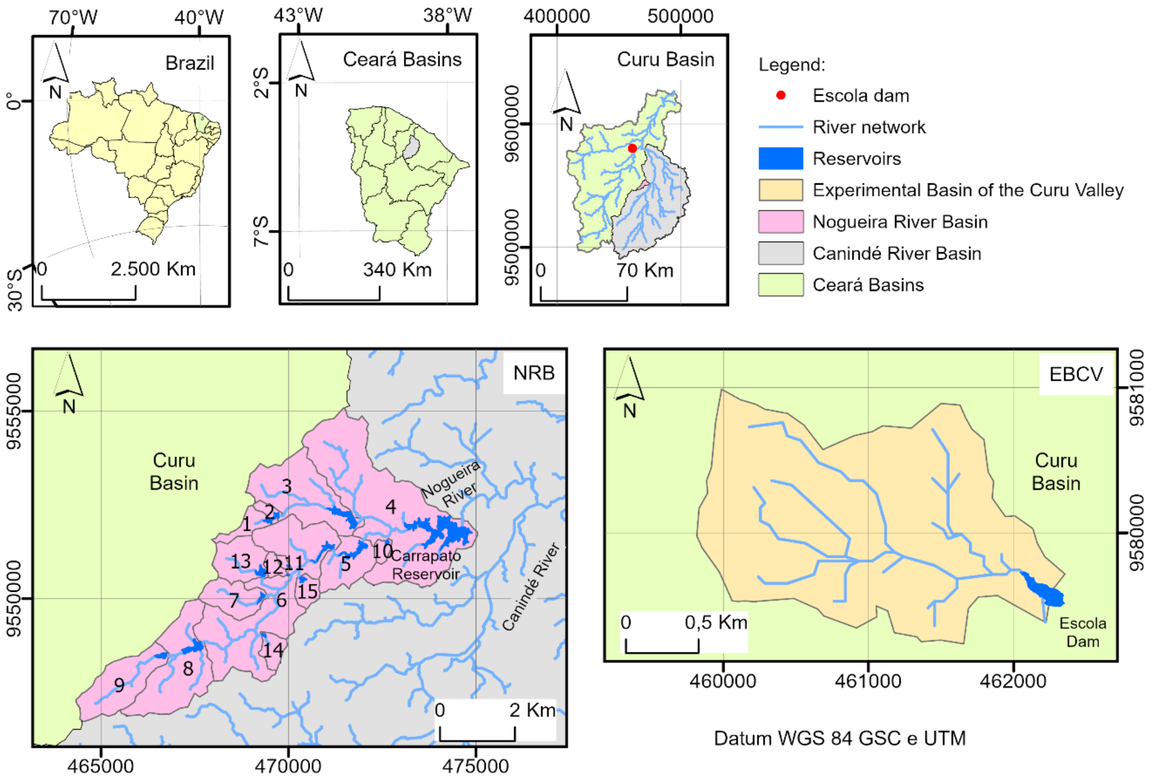


**Figure 1.** Location of the study area, highlighting the Experimental Basin of the Curu Valley (EBCV) and the Nogueira River Basin (NRB) with a network of 15 reservoirs.

The region has a hot and semiarid climate with irregular rainfall distributed from February to May, with an average annual precipitation of 801 mm, potential evapotranspiration of 2,130 mm/year. The predominant vegetation is degraded tree-shrub Caatinga (84% of the basin area), but other land uses are observed such as bare soil (5.9%), riparian forest (4.5%) and pasture and agriculture (1.8%). The basin has an elevation ranging from 65 to 208 m and flat terrain with slopes varying from 1 to 15%. The types of soil present in the area are orthic chromic luvisols (84%) and eutrophic haplic planosols (16%).

## 2.1. Estimation of dam failure risks in the reservoir network

To better understand the failure process of small dams in the semiarid region and the effects on the dynamics of sediment transport downstream, the Escola Dam, located at the EBCV outlet, was investigated in detail. The dam failed on April 23, 2020 as a result of a flood event with a return period of 41 years, according to the results obtained by De Menezes (2023). The geometric characteristics of the breach and the reservoir bed topography were captured to serve as a pilot study for the analysis of dam failures in the NRB.

The bed elevation changes in the Escola reservoir after failure and the volume of material eroded from the earth-fill dam body were estimated using Digital Elevation Model (DEM) based on the combination of three databases: a Topcon ES-105 total station used to detail the topography of the reservoir bed, focusing on the longitudinal profile following the water flow through the reservoir and some additional check and control points; a Global Navigation Satellite System (GNSS), with the Trimble R6 RTK GNSS, applied for spatial referencing of the points surveyed in the different bases; and a multirotor Remotely Piloted Aircraft (RPA) (DJI Mavic 2 Pro model), used to cover a larger area that includes the entire reservoir area and surroundings. DEMs generated in 2017 and 2021 (in this research) were then compared to estimate the total sediment erosion.

The cascade dam failures in the RNB was simulated using a combination of the HEC-HMS (Hydrologic Engineering Center - Hydrologic Modeling System; USACE, 2000) models in the simulation of the extreme flood events and HEC-RAS (Hydrologic Engineering Center - River Analysis System; USACE, 2016) in the simulation of the breach formation process during dam break. The characterization of the hydrological attributes of the NRB subbasins used as input data for the simulation with HEC-HMS was performed by processing altimetric data from the Copernicus database (European Space Agency, 2024), applying Geographic Information Systems (GIS) tools from the ArcGis Pro software. The time of concentration ($Tc$) in the NRB subbasins was calculated using the modified Kirpich equation (Equation 1), as follows:

$$Tc = 0{,}0663 \cdot CR^{0{,}77} \cdot S^{-0{,}385} \quad (1)$$

Where: $CR$ = length of the main river (km); $S$ = average slope of the main river (m m$^{-1}$).

Rainfall intensities were estimated using the intensity-duration-frequency (IDF) equation of the Pentecoste rainfall station (Equation 2), located very close to the reservoir within the UFC Experimental Farm (Rodrigues *et al.*, 2008). This equation was also applied to simulate extreme flood events in the NRB subbasins.

$$i = \frac{2246 \cdot Tr^{0{,}185}}{(D+18)^{0{,}95}} \quad (2)$$

Where: $i$ = rainfall intensity related to the concentration time for the RNB subbasins (mm h$^{-1}$); $Tr$ = return period (years); $D$ = rainfall duration of the event (min).

The failure of the NRB dams was then simulated using the HEC-RAS hydraulic model (Hydrologic Engineering Center - River Analysis System; USACE, 2016), considering the flood hydrograph generated with the HEC-HMS model as input data and the reservoir water level at the spillway crest elevation as initial condition. Furthermore, the breach characteristics were obtained in the field and complemented by information derived from the equations proposed by Froehlich (2008) for the development time (Equation 3) and the average breach width (Equation 4).

$$t_f = 63.2 \cdot \sqrt{\frac{V_w}{g\, h_b^{2}}} Tc = 0{,}0663 \cdot CR^{0{,}77} \cdot S^{-0{,}385} \quad (3)$$

$$B_{ave} = 0.27\, K_o\, V_w\, h_b^{0.04} Tc = 0{,}0663 \cdot CR^{0{,}77} \cdot S^{-0{,}385} \quad (4)$$

Where: $B_{ave}$ = average breach width (m); $K_o$ = a constant (1.3 for overtopping failures or 1.0 for piping); $V_w$ = reservoir volume at time of failure (m$^3$); $h_b$ = height of the final breach (m); g = gravitational acceleration ($m.s^{-1}$); and $t_f$ = breach formation time (s).

Sediment volume removed from the dam embankment during breach formation ($V_{eroded}$, in m³) was then estimated using Equation 5, proposed by MacDonald and Langridge-Monopolis for earth dam failures (Wahl, 1998), based on a sample of 42 reservoirs:

$$V_{eroded} = 0.0261(V_{out}h_w)^{0.769} t_f = 63.2 \cdot \sqrt{aa\frac{V_w}{g\,h_b{}^2}} Tc = 0{,}0663 \cdot CR^{0{,}77} \cdot S^{-0{,}385} \quad (5)$$

Where: $V_{out}$ = water volume of water passing through the breach (m³); and $h_w$ = water depth above the bottom of the breach (m). We assumed that $V_{out}$ is the volume of the reservoir at time of breach plus inflow volume after breach begins, minus any spillway and gate flow after breach begins. For that, a hydraulic simulation of water release through the spillway is performed to identify the peak of water discharge, as well as the maximum water level and volume selected as initial conditions for breach formation. To convert sediment volume into mass an average sediment density of 1.5 g $cm^{-3}$ was used as a reference value for earth-fill dams according to field measurements.

Based on the DEM for the reservoir area of the Escola Dam, generated using ground (GNSS and Total Station) and aerial (RPA) survey techniques, it was possible to characterize the reservoir bed topography and the breach geometry. The average breach width derived from topographic survey was 18.75 m, while the value computed using Equation 4 was 16.10 m. Furthermore, the volume of material eroded from the dam embankment during the breach formation was estimated by Equation 5 with a total of 1,136 m³ of remobilized material, slightly higher than the measured one (923 m³). These findings demonstrated the applicability of Equations 4 and 5 to simulate dam failures in small reservoirs (De Menezes, 2023).

**2.2. Estimation of sediment yield in the catchment**

For the estimation of sediment yield (SY) in the NRB, the Modified Universal Soil Loss Equation (MUSLE) was applied, as implemented in the WASA-SED (Water Availability in Semi-Arid environments – SEDiments) model (Mueller *et al.*, 2010; Mamede *et al.*, 2018) and presented in Equations 6 and 7:

$$SY = \chi\ K\ LS\ CP\ ATc = 0{,}0663 \cdot CR^{0{,}77} \cdot S^{-0{,}385} \quad (6)$$

$$\chi = 1.586\ (Q_{surf}\ Q_{peak})^{0.56}.A^{0.12} Tc = 0{,}0663 \cdot CR^{0{,}77} \cdot S^{-0{,}385} \quad (7)$$

Where: $\chi$ = rainfall energy term (MJ mm $ha^{-1}$ $h^{-1}$); $K$ = soil erodibility factor (t h $MJ^{-1}$ $mm^{-1}$); $LS$ = length-slope factor (-); $C$ = vegetation and crop management factor (-), $P$ the erosion control practice factor (-), $Q_{surf}$ is the surface runoff volume (mm); and $q_{peak}$ is the peak runoff rate (mm $h^{-1}$). The rainfall energy term $\chi$ of the MUSLE equation incorporates the surface and peak runoff, eliminating the need to enter a Sediment Delivery Ratio (SDR) as required in the Universal Soil Loss Equation (USLE), and implicitly accounts for antecedent soil moisture (Mueller *et al.*, 2010; Bronstert *et al.*, 2014). MUSLE has been successfully applied in studies on sediment production at the event scale worldwide (Gwapedza *et al.*, 2021; Hao *et al.*, 2022), including in semiarid basins in the State of Ceará (Mamede *et al.*, 2018).

For the parameterization of the sedimentological routine at the subbasin scale, the following data analysis and processing steps were performed:

i. Estimation of the rainfall energy term based on hydrological attributes of the NRB subbasins for the extreme flood events;

ii. Characterization of the soil erodibility factor (K) using measured data of soil properties in the region (Lira *et al.*, 2014);

iii. Mapping the terrain features in terms of the slope length factor (L) and slope factor (S) using Digital Elevation Model (DEM) derived from the Copernicus database (European Space Agency, 2024);

iv. Determination of the USLE cover and management factor C based on land cover characterization by using satellite images and field investigation. As no practice of protection against erosion was observed in the study area, the support practice factor P was set to 1;

v. Computation of sediment through the reservoir network applying a cascade scheme, where sediment input to a downstream reservoir comes from the catchment itself where it is located and from upstream reservoirs, including sediment discharges through their spillways and through their breaches whenever they fail. For convenience, sediment exchange between the water column and the riverbed downstream of the dams was disregarded;

vi. Estimation of sediment retention in the reservoir using a trap efficiency of 50%, as found by Mamede *et al.* (2018) for a network of 114 reservoirs with a range of surface areas varying from 0.003 to 350 ha.

## 3. RESULTS AND DISCUSSION

The simulation of cascade dam failures in the NRB was then carried out, with peak flows at the inlet (HEC-HMS) and outlet (HEC-RAS) of those reservoirs summarized in Table 1 for high return periods (50, 100, 1,000 and 10,000 years). Figure 2 illustrates the diagrams with reservoir network connections, highlighting the occurrence of cascade dam failures.

The results presented in Table 1 and Figure 2 show that only one reservoir (ID-5) failed at the 50-year peak flow, which can be explained by the fact that this reservoir has an undersized storage capacity and spillway geometry related to its large contribution area. Furthermore, it is positioned downstream in the reservoir network, receiving flows from several other reservoirs located upstream.

**Table 1.** Peak flows at the inlet (HEC-HMS) and outlet (HEC-RAS) of the NRB reservoirs for return periods of 50, 100, 1,000 and 10,000 years (highlighting dam failures in bold).

| Reservoir | Peak inflow ($m^3 s^{-1}$) | | | | Peak outflow ($m^3 s^{-1}$) | | | |
|---|---|---|---|---|---|---|---|---|
| | 50 | 100 | 1000 | 10000 | 50 | 100 | 1000 | 10000 |
| 1 | 9.2 | 11.0 | 19.3 | 32.3 | 6.2 | **56.6** | **67.2** | **80.6** |
| 2 | 7.7 | 58.3 | 71.9 | 90.8 | 6.8 | 31.3 | **79.4** | **96.3** |
| 3 | 40.8 | 69.1 | 123.0 | 169.9 | 23.9 | 34.7 | 69.5 | **669.7** |
| 4 | 659.3 | 833.6 | 972.0 | 1613.8 | 134.1 | 178.4 | **815.2** | **1359.2** |
| 5 | 105.7 | 378.4 | 517.4 | 835.0 | **664.9** | **755.2** | **892.2** | **1025.3** |
| 6 | 87.5 | 107.5 | 397.8 | 773.8 | 85.0 | **400.9** | **490.8** | **755.0** |
| 7 | 18.8 | 22.6 | 39.7 | 65.8 | 14.8 | 18.3 | 34.2 | **198.0** |
| 8 | 46.7 | 57.9 | 111.4 | 243.7 | 33.5 | 42.8 | 87.4 | **446.0** |
| 9 | 14.5 | 18.6 | 38.8 | 72.0 | 13.1 | 17.0 | 37.7 | **127.3** |
| 10 | 2.6 | 3.4 | 7.7 | 14.9 | 1.7 | 2.3 | 5.9 | 12.1 |
| 11 | 2.5 | 3.0 | 5.2 | 8.6 | 2.0 | 2.4 | 4.3 | 7.2 |
| 12 | 6.1 | 7.3 | 12.7 | 21.1 | 5.6 | 6.8 | 12.0 | **33.2** |
| 13 | 23.3 | 27.9 | 48.9 | 81.2 | 11.9 | 14.9 | 30.1 | **194.6** |
| 14 | 10.8 | 13.0 | 22.8 | 38.0 | 8.3 | 10.2 | **42.5** | **60.6** |
| 15 | 9.9 | 11.9 | 20.7 | 34.2 | 4.2 | 5.3 | 208.9 | **225.9** |

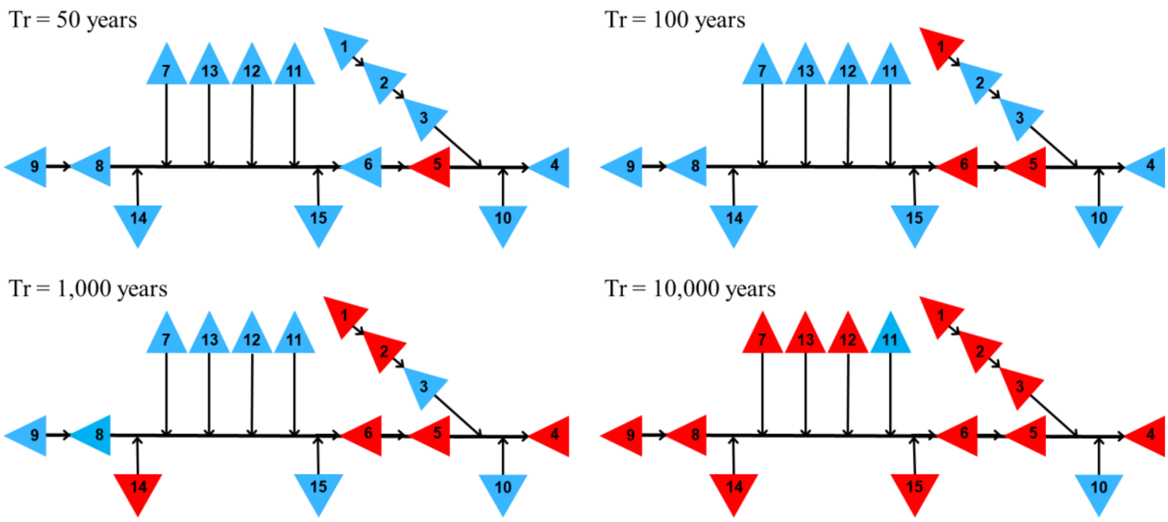


**Figure 2.** Diagrams with network connections of the NRB reservoirs, highlighting cascade dam failures for return periods of 50, 100, 1,000 and 10,000 years.

According to Figure 2, two reservoirs in the NRB (ID-10 and ID-11) did not fail even for extreme flood events with a return period of 10,000 years, which can be explained by the small area of their watersheds, resulting in flows lower than their spillway capacities of releasing water during flood events. It may also be observed that reservoirs located further downstream, when arranged in a cascade, are able to attenuate flood peaks resulting from failure of upstream dams, as observed in the cascade of dams ID-1, ID-2 and ID-3 (downstream to upstream). For the cascade of dams ID-5 and ID-4 (downstream to upstream), the largest reservoir in the network (ID-4), receives the flood hydrograph generated by failure of reservoir ID-5 for return periods up to 50 years, but only broke in simulations for extreme events related to return periods higher than 1,000 years, which is the usual condition for sizing dam spillways. According to the simulation results, six reservoirs would fail under this extreme condition. Other studies of cascade dam failures have considered different scenarios, such as the effect of an upstream dam failure on downstream dams without an associated flood event (Oliveira and Lima Neto, 2020) or with a single flood event with a 1,000-year return period (Campos and Saliba, 2023).

Sediment yield was computed by the sedimentological routine and sediment mass eroded from the dam embankment during the breach formation was derived from the simulations of cascade dam failures in the NRB using Equation 5. Then, the water and sediment routing through the reservoir network of the NRB was computed. The sediment budget for each reservoir is presented in Table 2, highlighting the occurrence of cascade dam failures and the increase in sediments resulting from erosion of the dam embankments. The results indicated a high mobilization of sediments from the dam embankment during the breach formation that are transported downstream, especially in more extreme events with a time period of 10,000 years. The amount of sediments eroded from the dam embankments for this extreme event (152,043 tons) is much higher than that yielded in the catchment area (11,456 tons), enhancing the negative effects of dam failure downstream in terms of sediment transport. According to Table 2, the sediment input into the outlet reservoir (ID-4) for a return period of 10,000 years was quite high (113,222 tons), derived from the catchment area (sediment yield) and from twelve dam failures upstream (sediment erosion from dam embankments). For this condition, this dam (ID-4) would also break, releasing a large amount of sediments downstream (163,483 tons).

**Table 2.** Sediment budget and routing through the NRB reservoir network for return periods of 50, 100, 1,000 and 10,000 years (highlighting dam failures in bold).

| Reservoir | Total sediment input (ton) | | | | Total sediment release (ton) | | | |
|---|---|---|---|---|---|---|---|---|
| | 50 | 100 | 1000 | 10000 | 50 | 100 | 1000 | 10000 |
| 1 | 48.3 | 62.1 | 133.0 | 260.3 | 24.1 | **711.7** | **1,089.1** | **1,621.7** |
| 2 | 33.7 | 724.5 | 1,119.3 | 1,684.7 | 16.9 | 362.2 | **2,024.9** | **2,926.4** |
| 3 | 374.1 | 811.5 | 2,929.6 | 4,623.7 | 187.1 | 405.7 | 1,464.8 | **16,832.6** |
| 4 | 16,063.4 | 30,439.2 | 50,467.5 | 113,221.8 | 8,031.7 | 15,219.6 | **89,266.6** | **163,483.1** |
| 5 | 525.3 | 11,420.8 | 22,868.8 | 57,329.9 | **15,573.0** | **29,637.3** | **48,121.4** | **94,616.0** |
| 6 | 975.1 | 1,231.8 | 5,440.8 | 28,868.8 | 487.6 | **11,370.6** | **22,751.4** | **57,085.7** |
| 7 | 160.4 | 204.9 | 430.0 | 830.1 | 80.2 | 102.4 | 215.0 | **3,713.3** |
| 8 | 316.9 | 407.0 | 869.6 | 4,523.8 | 158.4 | 203.5 | 434.8 | **13,861.8** |
| 9 | 109.4 | 150.3 | 378.7 | 827.2 | 54.7 | 75.2 | 189.3 | **3,231.9** |
| 10 | 1.3 | 2.5 | 12.1 | 37.4 | 0.7 | 1.3 | 6.1 | 18.7 |
| 11 | 4.2 | 5.7 | 14.4 | 31.5 | 2.1 | 2.9 | 7.2 | 15.8 |
| 12 | 26.4 | 35.3 | 83.0 | 173.3 | 13.2 | 17.6 | 41.5 | **551.2** |
| 13 | 188.8 | 242.5 | 516.1 | 1,006.2 | 94.4 | 121.2 | 258.1 | **4,174.8** |
| 14 | 46.8 | 61.9 | 142.2 | 292.0 | 23.4 | 31.0 | **576.7** | **968.1** |
| 15 | 66.0 | 86.8 | 196.4 | 399.0 | 33.0 | 43.4 | **2,515.5** | **3,017.1** |

The effects of cascading dam failures were then analyzed considering the average sediment concentrations at the reservoir inlet and outlet, as shown in Figures 3a and 3b, respectively. According to Figure 3a, it can be observed that the nine headwater reservoirs (ID-1, ID-7, ID-9, ID-10, ID-11, ID-12, ID-13, ID-14, ID-15) present a gradual increase in the incoming sediment concentration when the return period varies from 50 to 10,000 years. The other six reservoirs (ID-2, ID-3, ID-4, ID-5, ID-6, ID-8) located downstream in the RNB cascade, however, present abrupt changes in incoming sediment concentration resulting from failures in upstream dams, with mean values reaching 9.4 g $L^{-1}$. Figure 3b shows abrupt increases in sediment concentrations downstream of the dams for different return periods, indicating how dam failures affect the sediment dynamics through the reservoir network. In the simulation for a 10,000-year return period, the high impact on sediment concentration downstream can be observed, with failures of thirteen dams in the NRB reservoir network.

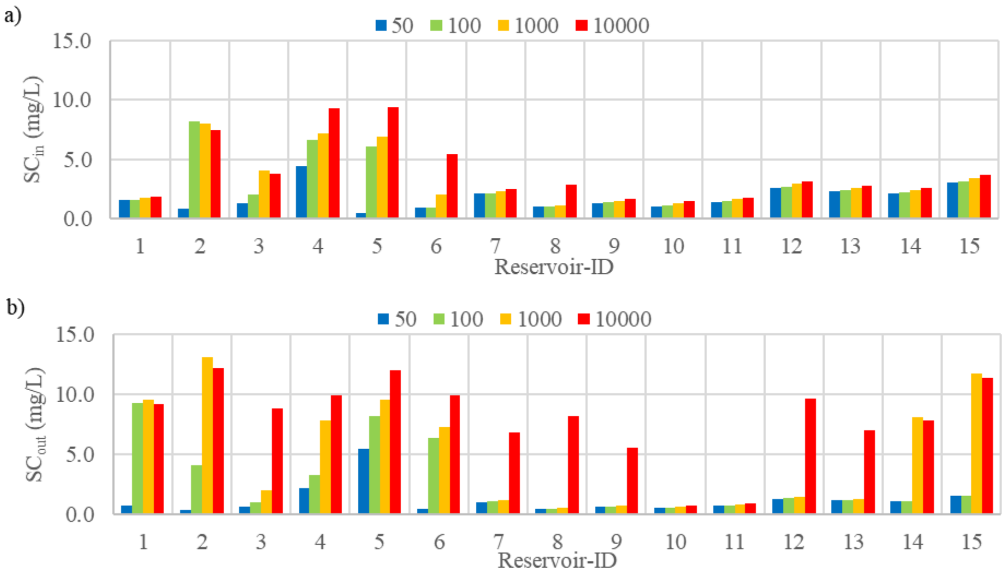


**Figure 3.** Average sediment concentrations at the reservoir inlet ($SC_{in}$) and outlet ($SC_{in}$) in the NRB, for return periods of 50, 100, 1,000 and 10,000 years.

Despite the uncertainties regarding the magnitude of extreme events and their erosive potential, as well as their ability to cause failures in cascade dams, some strategies were adopted to reduce these uncertainties, such as: the choice of a classical and widely applicable method for simulating sediment yield at the event scale such as MUSLE; the characterization of the breach geometry using equations tested for dam failure in the semi-arid region of Ceará such as the Escola dam; and the characterization of the spillway geometry carried out in situ to properly estimate its overflow release capacity and the occurrence of overtopping.

## 4. CONCLUSIONS

The main results of this study are highlighted below:

● The combined application of hydrological (HEC-HMS) and hydraulic (HEC-RAS) models allowed simulating the generation of the flood wave in the basin and analyzing the risks of cascade dam failure for different return periods (50 to 10,000 years), indicating that return periods greater than 100 years can result in cascade dam failures. It is important to highlight that this study only considered failure due to overtopping and, according to field observations, the safety conditions of the dams are very precarious, with presence of excessive vegetation, preventing the visualization of anomalies, making access to the dam structures difficult, impairing the drainage system, and creating preferred paths for percolation due to deep roots;

● Hydrological/hydraulic simulation performed on a network of small reservoirs indicated that extreme events associated with return times greater than 100 years can trigger cascading failures. The results also highlight the ability of larger reservoirs located downstream, when arranged in cascade, to attenuate flood waves resulting from failures of smaller dams located upstream. Nevertheless, they are still subject to failure for more extreme events (1,000 and 10,000 years);

● Cascade dam failures mobilize massive quantities of sediments eroded from the dam embankments, which are transported downstream and directly impact receiving water bodies, with greater severity for more extreme events (Tr = 10,000 years) and failures of thirteen NRB dams. The effects of dam failures can also be observed in abrupt changes in average sediment concentrations at the reservoir inlet and outlet, resulting from erosion of the dam embankments during breach formation.

## 5. DATA AVAILABILITY STATEMENT

Data availability not informed.

## 6. ACKNOWLEDGEMENTS

The authors acknowledge the Foundation for Scientific and Technological Development Support of Ceará (FUNCAP) for funding this research (Process n. UNI-0210-00025.01.00/23).

## 7. REFERENCES

ANA (Brasil). **Relatório de segurança de barragens 2024 - 2025**. Brasília, 2025.

BRONSTERT, A.; DE ARAÚJO, J. C.; BATALLA, R. J.; COSTA, A. C.; DELGADO, J. M.; FRANCKE, T. *et al.* Process-based modelling of erosion, sediment transport and reservoir siltation in mesoscale semi-arid catchments. **Journal of Soils and Sediments**, v. 14, n. 12, p. 2001-2018, 2014. https://doi.org/10.1007/s11368-014-0994-1

CAMPOS, R. G. D.; SALIBA, A. P. M. Methodology to evaluate cascade dams breaks for analysis and safety design. **Brazilian Journal of Water Resources**, v. 28, n. 16, 2023. https://doi.org/10.1590/2318-0331.282320230001

CHEN, H. J.; CUNNING, J. A practical tool for tailings dam breach analysis - numerical modelling of hydraulic erosion and discharge of flowable tailings. **Science of The Total Environment**, v. 980, n. 179467, 2025. https://doi.org/10.1016/j.scitotenv.2025.179467.

DE ARAÚJO, J. C.; MEDEIROS, P. H. A. Impact of dense reservoir networks on water resources in semiarid environments. **Australian Journal of Water Resources**, v. 17, p. 87-100, 2013.

DE MENEZES, S. K. M. **Ruptura de um pequeno reservatório no semiárido brasileiro e seus efeitos na topografia do leito.** 2023. 80f. Dissertação (Mestrado em Energia e Ambiente) - Universidade da Integração Internacional da Lusofonia Afro-Brasileira, Redenção-Ceará, 2023.

EUROPEAN SPACE AGENCY. **Copernicus Global Digital Elevation Model**. Distributed by OpenTopography. 2024. Available in: https://doi.org/10.5069/G9028PQB. Access: 2024 Jan. 01.

FROEHLICH, D. C. Embankment dam breach parameters and their uncertainties. **Journal of Hydraulic Engineering**, v. 134, n. 12, 1708-1720, 2008. http://dx.doi.org/10.1061/(ASCE)0733-9429(2008)134:12(1708)

FU, C.; ZHAO, T.; LI, H; HUO, D. Investigating the failure mechanisms of cascade landslide dams under overtopping conditions: an experimental approach. **Scientific Reports**, v. 15, n. 5835, 2025. https://doi.org/10.1038/s41598-025-89618-5

GWAPEDZA, D.; NYAMELA, N.; HUGHES, D. A.; SLAUGHTER, A. R.; MANTEL, S. K.; VAN DER WAAL, B. Prediction of sediment yield of the Inxu River catchment (South Africa) using the MUSLE. **International Soil and Water Conservation Research**, v. 9, n. 1, 37e48, 2021. https://doi.org/10.1016/j.iswcr.2020.10.003

GOMES, T. B. S. **Modelagem e Caracterização Geotécnica do solo da Barragem do Assentamento Olivencia localizada no Município de Quixadá/CE**. 2019. 89 f. TCC (Bacharelado em Engenharia Civil) – Universidade Federal do Ceará, Russas, 2019.

HAO, R.; HUANG, X.; CAI, Z. W.; XIAO, H. B.; WANG, J.; SHI, Z. H. Incorporating sediment connectivity index into MUSLE model to explore soil erosion and sediment yield relationships at event scale. **Journal of Hydrology**, v. 614, n. 128579, 2022. https://doi.org/10.1016/j.jhydrol.2022.128579y7

LIRA, D.; TOLEDO, C.; MAMEDE, G. Silting in the dense reservoir network of the Pereira de Miranda catchment. **Engenharia Agrícola**, v. 34, p. 671-682, 2014. https://doi.org/10.1590/S0100-69162014000400007

MAIA, L. P.; MAMEDE, G. L.; MEDEIROS, P. H. A.; DA SILVA, E. M. R.; VASCONCELOS, F. P.; SOARES, J. B. Políticas públicas na gestão integrada da zona costeira no Estado do Ceará: contribuições do Programa Cientista Chefe. **Revista DELOS**, v. 18, n. 64, e4206, 2025. https://doi.org/10.55905/rdelosv18.n64-151

MAMEDE, G. L.; ARAUJO, N.; SCNEIDER, C. M.; ARAÚJO, de J. C.; HERRMANN, H. J. Overspill avalanching in a dense reservoir network. **Proceedings of the National Academy of Sciences**, v. 109, n. 19, p. 7191-7195, 2012. https://doi.org/10.1073/pnas.1200398109

MAMEDE, G. L.; GUENTNER, A.; MEDEIROS, P. H. A.; DE ARAÚJO, J. C.; BRONSTERT, A. Modeling the Effect of Multiple Reservoirs on Water and Sediment Dynamics in a Semiarid Catchment in Brazil. **Journal of Hydrologic Engineering**, v. 23, n. 12, 2018. https://doi.org/10.1061/(ASCE)HE.1943-5584.0001701

MELLO, C. C. S.; ELEUTÉRIO, J. C. Assessing sediment dynamics and erosion-deposition patterns after a dam break: Insights from the Brumadinho tailings dam failure in Brazil, **Journal of South American Earth Sciences**, v. 157, p. 105472, 2025. https://doi.org/10.1016/j.jsames.2025.105472

MUELLER, E. N.; GUENTNER, A.; FRANCKE, T.; MAMEDE, G. L. Modelling sediment export, retention and reservoir sedimentation in drylands with the WASA-SED model. **Geoscientific Model Development**, v. 3, p. 275-291, 2010. https://doi.org/10.5194/gmd-3-275-2010

OLIVEIRA, L. C. S.; LIMA NETO, I. E. Simulação do rompimento de barragens em cascata em uma bacia hidrográfica semiárida. **Revista DAE**, v. 70, n. 235, p. 203-216, 2022.

PETER, S.; DE ARAÚJO, J. C.; ARAUJO, N.; HERRMANN, H. J. Flood avalanches in a semiarid basin with a dense reservoir network. **Journal of Hydrology**, v. 512, p. 408-420, 2014. https://doi.org/10.1016/j.jhydrol.2014.03.001

QIU, W.; LI, Y.; ZHANG, Y. WEN, L.; WANG, T.; WANG, J.; SUN, X. Numerical investigation on the evolution process of cascade dam-break flood in the downstream earth-rock dam reservoir area based on coupled CFD-DEM. **Journal of Hydrology**, v. 635, p. 131162, 2024. https://doi.org/10.1016/j.jhydrol.2024.131162.

RODRIGUES, J. O.; ANDRADE, E. M.; OLIVEIRA, T. S.; LOBATO, F. A. O. Equações de Intensidade – duração – frequência de chuvas para as localidades de Fortaleza e Pentecoste, Ceará. **Scientia Agraria**, v. 9, n. 4, p. 511-519, 2008.

TASKAYA, E.; BOMBAR, G.; TAYFUR, G. Experimental investigation of sediment movement as a result of homogeneous earth-fill dam overtopping break over a simplified urban area. **Journal of Hydrology**, v. 617, Part B, p. 128924, 2023. https://doi.org/10.1016/j.jhydrol.2022.128924

USACE. **HEC-HMS Hydrologic Engineering Center - Hydrologic Modeling System**. Technical Reference Manual, CPD-74B. US Army Corps of Engineers, 2000.

USACE. **HEC-RAS Hydrologic Engineering Center - River Analysis System**. User Manual. US Army Corps of Engineers, 2016.

VOSOUGHI, A.; RAKHSHANDEHROO, G.; NIKOO, M. R.; SADEGH, M. Experimental study and numerical verification of silted-up dam break. **Journal of Hydrology**, v. 590, 2020. https://doi.org/10.1016/j.jhydrol.2020.125267

WAHL, T. L. Prediction of embankment dam breach parameters - A literature review and needs assessment. **Dam Safety Rep. No. DSO-98-004.** Denver: U.S. Dept. of the Interior, 1998.

ZHANG, M.; WU, W.M. A two dimensional hydrodynamic and sediment transport model for dam break based on finite volume method with quadtree grid. **Applied Ocean Research**, v. 33, n. 4, p. 297-308, 2011. https://doi.org/10.1016/j.apor.2011.07.004

ZHAO, J.; OZGEN, I.; LIANG, D.; HINKELMANN, R. Comparison of depth-averaged concentration and bed load flux sediment transport models of dam-break flow. **Water Science and Engineering**, v. 10, p. 287-294, 2017. https://doi.org/10.1016/j.wse.2017.12.006